

Field Strength Correlators and Gluon Condensates at Finite Temperature from Renormalization Group Smoothing

Ernst-Michael Ilgenfritz¹ and Stefan Thurner²

¹*Institute for Theoretical Physics, Kanazawa University, Japan*

²*Institut für Kernphysik, TU-Wien, Austria*

Abstract

We summarize recent attempts to extract characteristics of non-perturbative vacuum structure from lattice measurements of the gauge invariant field strength correlator. As an alternative to cooling, we propose to apply the renormalization group (RG) smoothing method in lattice studies. For pure $SU(2)$ gauge theory we present magnetic and electric correlation lengths and condensates related to various correlators over a temperature range of $0.7 T_{\text{dec}} < T < 1.9 T_{\text{dec}}$.

PACS: 11.15.Ha, 12.38.Gc, 11.15.Kc, 11.10.Wx

I. INTRODUCTION

Quantum Chromodynamics (QCD) owes its confining property to non-perturbative structures of its groundstate which are, after many years of research, not yet uniquely identified. (for a recent overview of competing pictures see e.g. [1]). In a more pragmatic attitude, the Stochastic Vacuum Model (SVM) [2] describes the vacuum structure in terms of a few vacuum correlation functions and points out which are related to confinement. That only few correlators should characterize the vacuum is the consequence of a truncation of the hierarchy of correlation functions, essentially due to a postulate made within the SVM that the gauge fields are Gaussian random processes in Euclidean space-time. In this framework, the correlators enter, and relate to each other, various phenomenological predictions. Particularly interesting (exhausting, in the case of pure gluodynamics) is the gauge invariant gluon field strength correlator in Euclidean space (and its continuation to Minkowski space). According to the SVM, part of the Euclidean field strength correlator at zero temperature is related to the confinement property of the QCD ground state [3]. For heavy quarkonium states, the full correlator describes the effect of the gluon condensate on the level splitting in detail (see Ref. [4] and references therein). Wick-rotated to Minkowski space, the correlator serves to parametrize high energy hadron-hadron scattering (see e.g. Ref. [5]).

Regardless of how this truncation exactly works, these correlators incorporate the unknown non-perturbative mechanisms and can be considered as an implicit parametrization of the important gluonic vacuum field modes. If they were known, this information could be readily used to constrain the parameters of more explicit models of vacuum structure. The central role, both theoretically and phenomenologically, strongly suggests to extract the field strength correlator (and other vacuum correlators) from a first principle lattice simulation. It is interesting to notice that, although the SVM approach has been proposed more than a decade ago by Dosch and Simonov [2], on the lattice the field strength correlator has only been studied by the Pisa group. Apart from earlier results for $SU(2)$ [6] and $SU(3)$ [7] pure gauge theory, there are now precise results available, from an analysis using cooling, over an

interval of distances 0.1 ... 1.0 fm for pure $SU(3)$ gluodynamics [8,9], for QCD with dynamical (Kogut-Susskind) fermions [10] (four flavors, for two values of mass) over an interval 0.4 ... 1.0 fm, and, over the same interval of distances, for pure $SU(3)$ Yang-Mills theory very near the deconfining temperature [9].

Lattice data for $T = 0$ obtained and fitted in Refs. [8–10] give strong hints in favor of dominance of locally selfdual or antiselfdual field strengths. These data have been analyzed [11] from the point of view of the random instanton liquid model [12,13]. Here the following picture arises: a rather dilute liquid of instantons (with parameters which, in the case of full QCD, happen to be roughly consistent with parameters obtained from phenomenological analyses) can explain the field strength correlator, including the part which is believed to be responsible for confinement. The relevance of this statement for confinement is far from clear. Absolute confinement is, strictly speaking, a property of pure Yang-Mills theory alone. At this place let us mention that a much higher instanton density is extracted from the field strength correlator in the case of pure Yang-Mills theory than for full QCD [11].

On the other hand, according to a widespread opinion a random instanton liquid, however dense it might be, does not lead to an asymptotic string tension. This is obvious for calculations of the direct effect of the (unperturbed) instanton liquid on the static $Q-\bar{Q}$ potential via the Wilson loop. While the instanton potential rises linearly at intermediate distance, this does not correspond to the known string tension [14] if the phenomenological density and size are assumed to hold. Let us note, however, that neither instanton suppression by external charges or fields nor instanton interactions (see *e.g.* [15]) have been taken into account in these estimates. It has even been questioned [16] whether the available lattice evidence for confinement is conclusive at all. In short, in spite of the possibility of an instanton interpretation of the correlator, the role of instantons for confinement is still controversial. The answer depends on details of the modeling of the instanton liquid, in particular on the density and the shape of size distribution (see *e.g.* Refs. [17,18]).

There is an indirect route (not completely worked out yet) leading from the instanton liquid to confinement. It has been demonstrated that under certain circumstances an instan-

ton liquid induces the condensation (percolation) of magnetic monopoles (see Ref. [18] and earlier references therein) which should confine via a dual Meissner effect. A corresponding effective theory of a dual Abelian gauge field, interacting minimally with the (condensed) monopole field (Dual Abelian Higgs Model [19]) is characterized by the mass of the dual “photon” and a finite Higgs correlation length. Both quantities together determine [20] the gauge invariant non-Abelian field strength correlator which we are interested in. Therefore, in a more fundamental way, the two structure functions of the correlator at $T = 0$ are inherent to an infrared effective dual formulation of QCD (see also [21]).

Similarly to $T = 0$ the field strength correlator at finite temperature encodes information on generic non-perturbative structures of non-Abelian gauge field histories dominating the QCD partition function. In a similar spirit as of Ref. [11], the correlators obtained near the deconfinement transition in pure $SU(3)$ gauge theory [8,9] have been analyzed from the caloron (finite T instanton) point of view [22]. Such a description turns out to be possible only below the deconfinement temperature T_{dec} .

As any measurement involving the field strength, such lattice calculations are far from trivial. The cooling method has been used in most of the more recent studies. To our opinion, the implications of this method for the intended measurements have not been discussed thoroughly enough so far. In this paper, we are going to apply a different technique to improve the signal for extracting the field strength correlator from lattice gauge field ensembles. Our method is based on a (classically) perfect action and uses a renormalization group motivated smoothing procedure [23,24]. We shall give a presentation of first results obtained in this manner for finite temperature $SU(2)$ pure gauge theory. In contrast to $T = 0$, a similar splitting of correlation lengths related to the different structure functions is obtained with both techniques. Some possible differences should be closer examined whether they are due to the other gauge group $SU(2)$ used here, compared to $SU(3)$ analyzed with cooling. If not then, cooling would have a systematic effect concerning the relative strength of the structure functions \mathcal{D} and \mathcal{D}_1 at high temperature.

The paper is organized as follows. In Sec. II we give an introduction to the concept of

field strength correlators for zero and finite temperature; the correlators and their suitable decompositions into the structure functions are defined there. In Sec. III we briefly discuss the potential problems of the cooling method and recall in short the fixed point action renormalization group (RG) smoothing technique. In Sec. IV we describe our results, and conclude with a discussion in Sec. V.

II. FIELD STRENGTH CORRELATOR

The two-point field strength correlator is a non-local generalization of the gluon condensate, involving the field strength tensor at separate points :

$$\mathcal{D}_{\mu\rho\nu\sigma}(x) = g^2 \langle 0 | \text{Tr} \left\{ G_{\mu\rho}(0) S(0, x) G_{\nu\sigma}(x) S^\dagger(0, x) \right\} | 0 \rangle , \quad (1)$$

where $G_{\mu\rho} = T^a G_{\mu\rho}^a$ is the field strength, with T^a being the generators of the algebra of the color $SU(N_c)$ group in the fundamental representation. $S(x_1, x_2)$ is the (path ordered) Schwinger line (parallel transporter)

$$S(x_1, x_2) \equiv \text{P exp} \left(ig \int_{x_1}^{x_2} dz^\mu A_\mu(z) \right) , \quad (2)$$

with $A_\mu = T^a A_\mu^a$. It is necessary to include the non-Abelian Schwinger line phase factor in order to ensure gauge invariance. Usually the straight-line path from x_1 to x_2 is chosen to evaluate $S(x_1, x_2)$. The correlator describes the coherence of the gauge field (modulo gauge transformations) over some coherence length. This notion replaces the idea of “domains” originally imagined to form the gluon condensate. Completely contracted, it is the local gluon condensate defined as

$$G_2 \equiv \left\langle \frac{\alpha_s}{\pi} : G_{\mu\nu}^a G_{\mu\nu}^a : \right\rangle , \quad (\alpha_s = \frac{g^2}{4\pi}) , \quad (3)$$

which is obtained in the limit $|x_1 - x_2| \rightarrow 0$ from the regulated correlator.

A. Zero Temperature

At $T = 0$, Euclidean $O(4)$ invariance admits the decomposition (for $x = x_1 - x_2$)

$$\begin{aligned} \mathcal{D}_{\mu\rho\nu\sigma}(x) &= (\delta_{\mu\nu}\delta_{\rho\sigma} - \delta_{\mu\sigma}\delta_{\rho\nu}) [\mathcal{D}(x) + \mathcal{D}_1(x)] \\ &+ (x_\mu x_\nu \delta_{\rho\sigma} - x_\mu x_\sigma \delta_{\rho\nu} + x_\rho x_\sigma \delta_{\mu\nu} - x_\rho x_\nu \delta_{\mu\sigma}) \frac{\partial \mathcal{D}_1(x)}{\partial x^2}, \end{aligned} \quad (4)$$

where \mathcal{D} and \mathcal{D}_1 are two invariant functions (of Euclidean modulus $|x|$) containing information on the vacuum. The tensor structure related to \mathcal{D}_1 does not contribute to confinement, while $\mathcal{D} \neq 0$ is possible only in non-Abelian theories or in Abelian theories with monopoles.

It is convenient, in particular on the lattice, to define two other vacuum structure functions $\mathcal{D}_{\parallel}(x)$ and a $\mathcal{D}_{\perp}(x)$, according to whether the plaquettes defining the field strength component in question have one direction parallel to the 4-vector between the two points of observation. These functions are composed of \mathcal{D} and \mathcal{D}_1 as follows

$$\begin{aligned} \mathcal{D}_{\parallel} &\equiv \mathcal{D} + \mathcal{D}_1 + x^2 \frac{\partial \mathcal{D}_1}{\partial x^2}, \\ \mathcal{D}_{\perp} &\equiv \mathcal{D} + \mathcal{D}_1. \end{aligned} \quad (5)$$

The two basic vacuum structure functions at $T = 0$ have a non-perturbative and a perturbative part according to the notation

$$\begin{aligned} \mathcal{D}(x) &= \mathcal{D}^{np}(x) + \frac{a_0}{|x|^4} e^{-|x|/\lambda_0}, \\ \mathcal{D}_1(x) &= \mathcal{D}_1^{np}(x) + \frac{a_1}{|x|^4} e^{-|x|/\lambda_1}, \end{aligned} \quad (6)$$

Since the first structure function is closely related to confinement, the non-perturbative parts of the two functions are suggestively written as

$$\begin{aligned} \mathcal{D}^{np}(x) &= \frac{\pi^2}{6} \kappa G_2 \tilde{\mathcal{D}}(x), \\ \mathcal{D}_1^{np}(x) &= \frac{\pi^2}{6} (1 - \kappa) G_2 \tilde{\mathcal{D}}_1(x), \end{aligned} \quad (7)$$

where G_2 has to be identified with the gluon condensate (3) and

$$\tilde{\mathcal{D}}(0) = \tilde{\mathcal{D}}_1(0) = 1. \quad (8)$$

The so-called non-Abelianicity $\kappa = \mathcal{D}^{np}(0) / (\mathcal{D}^{np}(0) + \mathcal{D}_1^{np}(0))$ represents a certain fraction of the gluon condensate related to confinement. So far the functions $\tilde{\mathcal{D}}(x)$ and $\tilde{\mathcal{D}}_1(x)$ mostly have been fitted as exponential functions [7–10] of the modulus $|x|$

$$\tilde{\mathcal{D}}(x) = e^{-|x|/\Lambda_0} \quad \text{and} \quad \tilde{\mathcal{D}}_1(x) = e^{-|x|/\Lambda_1} , \quad (9)$$

although more physically motivated forms are available which fit the data as well [25].

In the SVM the string tension can be approximately related to the correlation length Λ_0 (coherence length of \mathcal{D}) and the gluon condensate [2],

$$\begin{aligned} \sigma &= \frac{1}{2} \int d^2x \mathcal{D}(x) \\ &= \frac{\pi^3}{12} \kappa G_2 \int dx^2 \tilde{\mathcal{D}}(x) = \frac{\pi^3}{6} \kappa G_2 \Lambda_0^2 . \end{aligned} \quad (10)$$

In the perturbative regime (at short distance) both \mathcal{D} and \mathcal{D}_1 behave as $1/|x|^4$. One-gluon exchange contributes only to the latter [26] giving $\mathcal{D}_1 = \frac{16}{3} \frac{\alpha_s}{\pi |x|^4}$. One-loop and higher order perturbative contributions to the string tension integral (10) are cancelled by higher correlator contributions [27].

Purely selfdual or antiselfdual non-perturbative background fields contribute only to \mathcal{D} (see Ref. [28,11]). In this case, it is the overlap of different selfdual or antiselfdual configurations (higher order contributions in an expansion in the density [11]) which generates the non-perturbative part of \mathcal{D}_1 . The observation that $\mathcal{D} \gg \mathcal{D}_1$, first made for $T = 0$ lattices, supports the idea that strong fields are dominantly selfdual or antiselfdual.

It was only for $T = 0$ that the newer data have been analyzed by the authors themselves [8–10]. As short distances became observable at higher β it has been confirmed that the functions \mathcal{D} and \mathcal{D}_1 contain a perturbative part which could be subtracted by a fit like (6). For the case of quenched $SU(3)$ gauge theory the two correlation lengths have been found equal, $\Lambda_0 \approx \Lambda_1 \approx 0.22$ fm. ¹ The data for full QCD show that the correlation length Λ_0 becomes smaller with increasing quark mass towards the quenched case. For the chiral limit an upper limit for the correlation length can be estimated as $\Lambda_0 \approx \Lambda_1 \approx 0.45$ fm. The gluon condensate G_2 as extracted from the correlator according to (6,7) is much larger in pure Yang-Mills theory than any phenomenological value.

¹For quenched $SU(2)$ gauge theory, a first analysis [6] without cooling has found $\Lambda_0 \approx 0.17$ fm.

In Ref. [11] the field strength correlator data at intermediate distance have been used to extract the two parameters characterizing the random instanton liquid model [12] which gives a good description of most of the hadronic correlators at zero temperature.² The size distribution of this model is approximated as $d(\rho) = \delta(\rho - \bar{\rho})$, so density n_4 and size $\bar{\rho}$ are the only parameters. The investigation in Ref. [11] was carefully dealing with the path dependence of the Schwinger factor in the instanton background. For a straight line path, a reasonable description over the measured range of distances has been achieved with parameters roughly compatible with phenomenological estimates where this is possible: density $n_4 = 0.5 \text{ fm}^{-4}$ and size $\bar{\rho} = 0.44 \text{ fm}$ for full QCD (with four flavors), to compare with $n_4 = 4 \text{ fm}^{-4}$ and $\bar{\rho} = 0.3 \text{ fm}$ in pure $SU(3)$ Yang-Mills theory. Second order terms in n_4 give subleading contributions to \mathcal{D} and are the leading ones in \mathcal{D}_1 . As long as deviations from selfduality or antiselfduality are entirely due to II , $\bar{I}\bar{I}$ and $I\bar{I}$ overlap, this analysis has led to the conclusion that $\mathcal{D}_1 < 0$ is characteristic for the instanton liquid at $T = 0$. Although this was not the case in the original fit given by the authors, it has been shown that the quenched data [8,9] are compatible with a small negative \mathcal{D}_1 as well. With the second order terms taken into account for pure Yang-Mills theory, the best fit leads to a change towards smaller $n_4 = 3.4 \text{ fm}^{-4}$ and $\bar{\rho} = 0.27 \text{ fm}$. The smallness of the correction *a posteriori* justifies the dilute gas approach to pure Yang-Mills theory and even more so for full QCD. As a rule one can summarize that instanton radii estimated in this way are 20 % to 30 % bigger than the (exponential) correlation length of \mathcal{D} .

²Strictly speaking, with the classical shape of an instanton in the trivial vacuum the asymptotic behavior at $x^2 \rightarrow \infty$ of the correlator $\mathcal{D}(x)$ can not be described. The inclusion of the interaction with the vacuum medium into the “classical” Euclidean field equation results in a modified instanton profile far from the center [29]. For a recent interesting attempt to find a modified instanton solution and to use it for the correlator see Ref [30].

B. Finite Temperature

At finite temperature, the $O(4)$ space-time symmetry is broken to the spatial $O(3)$ symmetry and the number of independent correlators is enlarged [31]. All of them separately depend on $|\mathbf{x}_1 - \mathbf{x}_2|$ and $(x^4)_1 - (x^4)_2$. We consider

$$\begin{aligned} \langle 0|Tr\{E_i(x_1)S(x_1, x_2)E_j(x_2)S^\dagger(x_1, x_2)\}|0\rangle = \\ \delta_{ij} \left(\mathcal{D}^E + \mathcal{D}_1^E + x_4^2 \frac{\partial \mathcal{D}_1^E}{\partial x_4^2} \right) + x_i x_j \frac{\partial \mathcal{D}_1^E}{\partial \mathbf{x}^2}, \end{aligned} \tag{11}$$

where $E_i = G_{i4}$ is the electric field, and

$$\begin{aligned} \langle 0|Tr\{B_i(x_1)S(x_1, x_2)B_j(x_2)S^\dagger(x_1, x_2)\}|0\rangle = \\ \delta_{ij} \left(\mathcal{D}^B + \mathcal{D}_1^B + \mathbf{x}^2 \frac{\partial \mathcal{D}_1^B}{\partial \mathbf{x}^2} \right) - x_i x_j \frac{\partial \mathcal{D}_1^B}{\partial \mathbf{x}^2}, \end{aligned} \tag{12}$$

where $B_i = \frac{1}{2} \epsilon_{ijk} G_{jk}$ is the magnetic field. Let us assume that $x = (0, 0, |\mathbf{x}|, 0)$ and define longitudinal and transversal correlators for electric and magnetic fields

$$\mathcal{D}_{\parallel}^E = \mathcal{D}^E + \mathcal{D}_1^E + \mathbf{x}^2 \frac{\partial \mathcal{D}_1^E}{\partial \mathbf{x}^2} \quad (i = j = 3 \text{ in eq.(11)})$$

$$\mathcal{D}_{\perp}^E = \mathcal{D}^E + \mathcal{D}_1^E \quad (i = j = 1, 2 \text{ in eq.(11)})$$

(13)

$$\mathcal{D}_{\parallel}^B = \mathcal{D}^B + \mathcal{D}_1^B \quad (i = j = 3 \text{ in eq.(12)})$$

$$\mathcal{D}_{\perp}^B = \mathcal{D}^B + \mathcal{D}_1^B + \mathbf{x}^2 \frac{\partial \mathcal{D}_1^B}{\partial \mathbf{x}^2} \quad (i = j = 1, 2 \text{ in eq.(12)}) .$$

In addition there is an electric-magnetic correlator which will not be considered here.

As a first step, in Ref. [22] an exponential plus perturbative fit in terms of $\mathcal{D}^{E,B}$ and $\mathcal{D}_1^{E,B}$ has been tried to describe the finite T quenched $SU(3)$ correlator measured in [9] with cooling

(which is known at distances > 0.4 fm). For the magnetic correlators, immediately below the deconfining transition, at a temperature $T = 0.978 T_{\text{dec}}$, the two structure functions have clearly different correlation lengths, $\Lambda_0^B = 0.19$ fm and $\Lambda_1^B = 0.53$ fm. The first one slowly increases across the transition, while the second goes through a maximum there. For the two electric structure functions at the temperature $T = 0.978 T_{\text{dec}}$, different correlation lengths $\Lambda_0^E = 0.17$ fm and $\Lambda_1^E = 0.41$ fm have been found, too. These fits show a tendency for both electric correlation lengths to drop suddenly at the transition. Unfortunately, there is no cooling data for pure $SU(2)$ at finite temperature that would allow a more direct comparison. A description using the Harrington-Shepard caloron solution, i.e., the periodic instanton [32,33], is the main objective in Ref. [22]. Below the deconfinement temperature, where $\mathcal{D}^B \approx \mathcal{D}^E$ and $\mathcal{D}_1^B \approx \mathcal{D}_1^E$ has been found and where $\mathcal{D}^{E,B} \gg \mathcal{D}_1^{E,B}$, a satisfactory description of magnetic and electric correlators was possible using these selfdual or anti-selfdual configurations while the small differences could be attributed to overlapping two-caloron (or caloron-anticoloron) configurations. The ratio $\mathcal{D}_1^E/\mathcal{D}^E$ strongly increases above the transition.

After describing our smoothing method in the next section, we will discuss the correlation lengths for the different finite temperature structure functions according to exponential Ansätze similar to what has been done in Ref. [22] for the cooled $SU(3)$ data, making combined fits to electric and magnetic data separately, in terms of \mathcal{D}^E and \mathcal{D}_1^E and in terms of \mathcal{D}^B and \mathcal{D}_1^B , respectively. We will also discuss a fit which directly applies to the *raw data* for $\mathcal{D}_{\parallel}^E$ and \mathcal{D}_{\perp}^E simultaneously, as well as for $\mathcal{D}_{\parallel}^B$ and \mathcal{D}_{\perp}^B . In this case we will separate the data into \mathcal{D} and \mathcal{D}_1 afterwards, using the obtained form of the fit. It should be emphasized already here that, due to our smoothing method, these functions are obtained essentially free of a perturbative contribution.

III. LATTICE METHODS

A. Smoothing vs. Cooling

The Pisa group [7–10] has used the cooling method in order to measure the field strength correlators at $T = 0$, both without external sources (in vacuum) and in the presence of an external Wilson loop [34],³ and at temperature near T_{dec} . For the measurement, similar to the search for instantons, it turned out necessary to eliminate ultraviolet fluctuations. It has been argued that, due to the diffusive nature of cooling, the correlator to be measured at a distance da ($a =$ lattice spacing) would not be affected before a number $n_{\text{cool}} \propto d^2$ of cooling iterations would have been performed. Practically, one measures the expectation values defining $\mathcal{D}_{\parallel}(da)$ and $\mathcal{D}_{\perp}(da)$ as a function of n_{cool} . The actual correlator is then defined as the plateau value *vs.* n_{cool} . Although it has not been presented in detail, experience seems to justify the expectation that this plateau is reached safely before $|x_1 - x_2|$ happens to fall within the diffusion radius $d \propto \sqrt{n_{\text{cool}}}$. In another context it has been shown that this amount of cooling amounts to a renormalization of coupling, which is expected to show up in the perturbative signal contributing to the correlator.

If cooling is technically necessary to improve the signal-to-noise ratio, one could be concerned to what extent it distorts the non-perturbative modes that existed in the true vacuum, i.e., to what extent the correlation lengths and the strength of the correlators are affected by the procedure itself. Since the (exponential) correlation length of the correlator \mathcal{D} is even smaller than the phenomenological instanton size it is useful to recall what effect cooling has in the attempt to fix instanton size and density from analyzing the topological density of a configuration. For this purpose, the cooling technique nowadays is superseded by adopting two, essentially opposite extreme ways to control that effect. The first prescription requires to observe the average size as function of n_{cool} , extrapolating it backward to zero cooling steps [36] in order to obtain the would-be instanton size in vacuum. The other uses a

³Bali et al. [35] have analyzed the correlator in the presence of external charges, analyzing quenched lattice data for heavy quark forces adopting certain factorization assumptions from SVM.

global stopping criterion [37] requiring cooling to be stopped when the density of instantons becomes equal to the (much better known!) topological susceptibility. This second method implicitly adopts a non-interacting instanton gas picture, which differs principally from the instanton liquid. It is recognized by now that one has to control cooling since instantons, once they become discernible by cooling or smearing, are steadily growing, becoming more and more classical, while small size instanton-antiinstanton pairs annihilate. Improved cooling [38] aims to stabilize instantons with $\rho > \rho_{\min}$, still suffering from the latter problem. Presently, there is no method agreed upon, such that the instanton size cannot be uniquely defined on the lattice [39]. Each of the methods seems to have a smoothing radius of the lattice fields (depending on n_{cool}) which should be well below the distances at which one measures the correlator. ⁴

During the last two years a method has been advocated [23,24] that avoids propagating, iterative procedures to suppress UV fluctuations. Alternatively, it uses first blocking and subsequent inverse blocking with respect to a perfect action in order to accomplish the necessary smoothing of equilibrium configurations, while it preserves their long range structure beyond the smoothing scale. So far, this method has been used exclusively to analyze the instanton [23] and monopole structure [23,24,41] of Monte Carlo generated configurations. As for monopoles, smoothing wipes out small monopole loops which are irrelevant for confinement (similar to blockspin renormalizations directly applied to the magnetic currents [42,18]).

B. Smoothing with a Perfect Action

To carry out a theoretically and technically consistent analysis, one has to implement a fixed point (FP) action. The simplified fixed-point action [43] for $SU(2)$ has been improved

⁴Very recently a local stopping criterion for cooling has been proposed [40] that seems to accomplish a tunable, well-defined smoothing radius.

recently, and a suitably truncated version [44] has been obtained. It is also parametrized in terms of only two types of Wilson loops, plaquettes (type C_1)

$$U_{C_1} = U_{x,\mu,\nu} = U_{x,\mu} U_{x+\mu,\nu} U_{x+\nu,\mu}^+ U_{x,\nu}^+ \quad (14)$$

and tilted 3-dimensional 6-link loops (type C_2) of the form

$$U_{C_2} = U_{x,\mu,\nu,\lambda} = U_{x,\mu} U_{x+\mu,\nu} U_{x+\mu+\hat{\nu},\lambda} U_{x+\nu+\hat{\lambda},\mu}^+ U_{x+\lambda,\nu}^+ U_{x,\lambda}^+ , \quad (15)$$

and contains several powers of the linear action terms corresponding to each loop (of both types) that can be drawn on the lattice

$$S_{FP}(U) = \sum_{i=1}^2 \sum_{C_i} \sum_{j=1}^4 w(i, j) \left(1 - \frac{1}{2} \text{Tr} U_{C_i}\right)^j . \quad (16)$$

The parameters of this action as used in this work are reproduced in Table I. A comparison reported in detail in [24] shows that the new parametrization is near to perfect.

With this action at hand one can now proceed to perform renormalization group transformations on the lattice. Suppose we have a fine lattice of links U and a coarse lattice of links V covering the same physical volume. Being a classically perfect action, S_{FP} can be evaluated on both lattices and must satisfy the following condition

$$\text{Min}_U (S_{FP}(U) + \kappa T(U, V)) = S_{FP}(V) , \quad (17)$$

configuration by configuration over a representative ensemble of equilibrium gauge field configurations V , each in one-to-one correspondence to a fine configuration U saturating the lower bound on $S_{FP}(U) + \kappa T(U, V)$ provided by the right hand side. $T(U, V)$ is a certain non-negative functional related to the blockspin transformation (see [43,23]). Eq. (17) can be read as the saddle point equation for an integral over fine configurations defining the blocked action $S_{FP}(V)$. Neglecting the one-loop corrections is justified in the classical limit for $\beta \rightarrow \infty$. The parameter $\kappa = 12.0$ (not to be confused with the non-Abelianicity factor mentioned above) has been fixed in the context of the adopted blocking scheme by an optimization of the locality properties of the quadratic part of the action.

Blocking means a mapping from the link fields U on the fine lattice to link variables V which describe the same configuration on the next coarser length scale. This mapping is accomplished by the following construction:

$$\begin{aligned} \tilde{V}_{x,\mu} = & c_1^{block} U_{x,\mu} U_{x+\hat{\mu},\mu} \\ & + \sum_{\nu \neq \mu} c_2^{block} \left(U_{x,\nu} U_{x+\hat{\nu},\mu} U_{x+\hat{\nu}+\hat{\mu},\mu} U_{x+2\hat{\mu},\nu}^+ + U_{x-\hat{\nu},\nu}^+ U_{x-\hat{\nu},\mu} U_{x-\hat{\nu}+\hat{\mu},\mu} U_{x-\hat{\nu}+2\hat{\mu},\nu} \right) . \end{aligned}$$

The coarse link variable $V_{x,\mu}$ is obtained by normalization to a $SU(2)$ group element $V_{x,\mu} = \tilde{V}_{x,\mu} / \sqrt{\det(\tilde{V}_{x,\mu})}$. The blocking parameters $c_2^{block} = 0.12$ and $c_1^{block} = 1 - 6 c_2^{block}$ have been optimized earlier in Ref. [45] under rather general conditions.

Inverse blocking is a mapping $V \rightarrow U^{SM}$ where the new link variables $U = U^{SM}$ are implicitly defined as the set of links providing, for the configuration encoded in V , the “smoothest interpolation” on the next finer grained lattice. Practically, the link field U^{SM} is found by minimizing the extended action on the left hand side of Eq. (17). This is not a truly classical field on the lattice but it is smoother than any quantum field U that could give rise to the coarse level field V . Technically speaking, κ plays here a role similar to a Lagrange multiplier defining the strength of the constraint imposed by the coarse grained configuration.

The $SU(2)$ pure gauge field configurations to be analyzed below have been generated on a $12^3 \times 4$ lattice at various β with the (classical) perfect action. In Ref. [24] we have localized the deconfinement phase transition at $\beta_c = 1.545(10)$. Corresponding to the second order character of that phase transition, the intersection of Binder cumulants of Polyakov loops for different $3d$ lattice volumes had been used for this purpose. Although the simulation was done on the fine lattice, the Binder cumulants built from V lattice Polyakov loops give the same β_c . While the Polyakov line correlators become critical at the transition, the various field strength correlation lengths remain finite across the transition.

C. Measuring the Field Strength Correlators

Here we demonstrate how we can get immediate access to the non-perturbative part of the field strength correlators applying the RG smoothing method. With some reservations, the results can be compared with cooling analyses (unfortunately available only for $SU(3)$). The field strength components $g a^2 G_{\mu\nu}(x)$ are defined as the average of the antihermitean part $\frac{1}{2i} (U_{x,\mu,\nu} - U_{x,\mu,\nu}^+)$ of the four equal-oriented ‘‘clover leaf’’ plaquettes in the $\mu\nu$ plane which are open at the lattice site x :

$$g a^2 G_{\mu\nu}(x) = \frac{1}{8i} (U_{x,\mu,\nu} + U_{x,\nu,-\mu} + U_{x,-\mu,-\nu} + U_{x,-\nu,\mu} - \text{h.c.}) . \quad (18)$$

For the purpose of the following study we take advantage of the fact that in the result of smoothing, similar to cooling, the renormalization constant becomes $Z \approx 1$ for the gluon fields.

We have measured only equal-time correlators, *i.e.* with a timelike argument $(x^4)_1 - (x^4)_2 = 0$. For lattice sites x_1, x_2 separated not along one of the spacelike axes, the choice of the Schwinger line is not unique. In that case averaging of expression (1) has been performed over a random selection of ten shortest paths connecting x_1 and x_2 , each path defining an independent transporter $S(x_1, x_2)$. Naturally, for $\mathcal{D}_{\parallel}^E$, $\mathcal{D}_{\parallel}^B$, \mathcal{D}_{\perp}^E , and \mathcal{D}_{\perp}^B , the field components \mathbf{E}_{\parallel} , \mathbf{B}_{\parallel} , \mathbf{E}_{\perp} and \mathbf{B}_{\perp} parallel or perpendicular to the 3-vector $\mathbf{x}_1 - \mathbf{x}_2$ have been appropriately projected out of the field strength tensor $G_{\mu\nu}$.

IV. RESULTS

The raw data for $\beta = 1.4$ and $\beta = 1.5$ (confinement), for $\beta = 1.55$ (just above deconfinement) and three temperatures in the deconfined phase ($\beta = 1.6$, $\beta = 1.7$ and $\beta = 1.8$) are shown in Fig. 1, together with an ad hoc fit to be discussed below. The two correlation functions \mathcal{D}_{\perp}^E and $\mathcal{D}_{\parallel}^B$ have to be understood as averages over two correlators involving mutually parallel components of \mathbf{E} or \mathbf{B} orthogonal to $\mathbf{x}_1 - \mathbf{x}_2$. For better visibility the sum is shown in Fig. 1. The data shown are averaged over correlators with exactly equal

distance. Even then the data still would show an eventual rotational non-invariance (in the three-dimensional distance) if rotational symmetry would be seriously broken.

A. Two-Exponential Fit

At first, analogously to the procedure of DiGiacomo et al. applied to their $T = 0$ cooled data [8–10], we have adopted the decomposition (13) into the basic structure functions for the \mathbf{E} and \mathbf{B} correlators separately, here however without a perturbative part which is suppressed by the steps of blocking and inverse blocking (see Sec. IV.B). We have assumed the following form for the basic \mathbf{E} and \mathbf{B} correlators

$$\mathcal{D}(\mathbf{x}) = A_0 e^{-|\mathbf{x}|/\Lambda_0},$$

$$\mathcal{D}_1(\mathbf{x}) = A_1 e^{-|\mathbf{x}|/\Lambda_1}.$$

Only correlator data at distances $d \geq 2a$ have been included into the fit, in accordance to our understanding that fields below that scale are interpolated in a smooth way and taking the extendedness of the field strength operator (18) into account. The four corresponding parameters are given in Table II to allow a comparison with the amplitudes and exponential correlation lengths obtained for $T \approx T_{\text{dec}}$ by the cooling method for $SU(3)$ [9] as analyzed in Ref. [22].

First, we mention that all structure functions are found positive at these temperatures in both cases. This property is corroborated also in the second way of fitting to be discussed below. Generally, at all temperatures, the two-exponential fit does not properly describe the decay of $\mathcal{D}_{\parallel}^B$ as measured here by the smoothing method at the largest distances. Due to cancellation in the expression

$$\mathcal{D}^B + \mathcal{D}_1^B + \mathbf{x}^2 \frac{\partial \mathcal{D}_1^B}{\partial \mathbf{x}^2}$$

this function would drop too fast. The two correlation lengths associated with \mathcal{D}^B and \mathcal{D}_1^B by the fit are almost degenerate and do not grow with temperature.

For the \mathbf{E} correlators, a correlated fit of $\mathcal{D}_{\parallel}^E$ and \mathcal{D}_{\perp}^E starts to be increasingly inadequate at temperatures $T > T_{\text{dec}}$. An indication is the \mathbf{E} correlator amplitude A_0 for $T = 1.15 T_{\text{dec}}$ where the signal has an uncertainty of the same order of magnitude. Taking the parameters of this fit seriously, the most dramatic feature is the drop of the correlation length of \mathcal{D}^E across the phase transition. At $\beta = 1.4$ ($T = 0.71 T_{\text{dec}}$), safely below the deconfining transition, we observe a weak splitting of the two correlation lengths, with $\Lambda_0 \approx 0.22$ fm. At $T = 0.9 T_{\text{dec}}$ we find still $\Lambda_0 \approx 0.18$ fm. Immediately above the deconfining transition (at $T = 1.02 T_{\text{dec}}$) it has dropped already to 0.10 fm.

B. Gauss-Exponential Fit

For the purpose of the fit shown in Fig. 1, we assumed all four functions to have a form like $A \exp(-B |\mathbf{x}| - C |\mathbf{x}|^2)$ and required the same limit for $|\mathbf{x}| \rightarrow 0$ for $\mathcal{D}_{\parallel}^E$ and \mathcal{D}_{\perp}^E , as well as for $\mathcal{D}_{\parallel}^B$ and \mathcal{D}_{\perp}^B .

In addition to this, have we considered remaining perturbative contributions to these four functions being proportional to $1/|\mathbf{x}|^4$. For all temperatures and all correlation functions we found this contribution to be smaller than the signal by one or two orders of magnitude over the range of distances from 1 to 6 lattice spacings. Of course, also here only correlator data at distances $d \geq 2 a$ have been included into the fit. In the following we therefore only discuss parameters which were determined by fits neglecting such a power-like perturbative contribution.

The parameters A , B , and C are listed in Table III in lattice units. In the confinement phase, the coefficient C is relatively important only for $\mathcal{D}_{\parallel}^E$ and \mathcal{D}_{\perp}^B . While it remains roughly unchanged also at higher temperature for the magnetic correlator, it rises dramatically in the electric case in order to account for the rapid decay. On the basis of this fit, we have determined the structure functions \mathcal{D}^E , \mathcal{D}_1^E , \mathcal{D}^B and \mathcal{D}_1^B which are shown in Fig. 2 for all β values.

In a first step the $\mathcal{D}_1^{E,B}$ have been numerically obtained by integrating the difference

$\mathcal{D}_{\parallel}^{E,B} - \mathcal{D}_{\perp}^{E,B}$ (as represented by the fits) from 0 to $|\mathbf{x}|$. The integration constants $\mathcal{D}^{E,B}(0)$ are fixed by the condition that $\mathcal{D}_1 \rightarrow 0$ for $|\mathbf{x}| \rightarrow \infty$. We find the functions $\mathcal{D}_1^{E,B}$ positive. Finally, the $\mathcal{D}^{E,B}$ have been obtained subtracting $\mathcal{D}_1^{E,B}$ from $\mathcal{D}_{\perp}^{E,B}$.

The amplitudes $\mathcal{D}^E(0)$, $\mathcal{D}_1^E(0)$, $\mathcal{D}^B(0)$, $\mathcal{D}_1^B(0)$ (which are related to the gluon condensate at high temperature) and the integrated correlation lengths of \mathcal{D}^E and \mathcal{D}^B , $\xi_{int}^{E,B} = \int_0^{\infty} d|\mathbf{x}| \mathcal{D}^{E,B}(\mathbf{x}) / \mathcal{D}^{E,B}(0)$, are given in Table IV for the six temperatures. As long as $T < T_{dec}$ the functions $\mathcal{D}_1^{E,B}$ are smaller by roughly a factor four than the corresponding $\mathcal{D}^{E,B}$. That means that selfdual or antiselfdual fields are less dominant in this range of temperatures compared to zero temperature. The ratio $\mathcal{D}_1/\mathcal{D}$ has been found [22] considerably smaller below the deconfinement transition in an analysis of $SU(3)$ correlators obtained with cooling. Since there are no cooling data for $SU(2)$ so far in our temperature range, we cannot decide whether this is due to the other gauge group or whether there is a systematic effect of cooling to enhance the contribution of locally (anti)selfdual configurations to the correlator at higher temperature but still in the confined phase.

The condensates $\mathcal{D}^E(0)$ and $\mathcal{D}^B(0)$ only slightly grow across the transition and start to rapidly grow not before $T > 1.2 \dots 1.5 T_{dec}$. Up to these temperatures the $\mathcal{D}_1^{E,B}(0)$ have increased to a size comparable with $\mathcal{D}^{E,B}(0)$.

The integrated correlation lengths of $\mathcal{D}^{E,B}$ shrink in a rather continuous way over the temperature range considered from 0.3 fm (electric and magnetic) at $T = 0.7 T_{dec}$ to 0.13 fm (magnetic) and 0.07 fm (electric) at $1.9 T_{dec}$ (Fig. 3). The smooth change of the four structure functions with increasing temperature is shown in Fig. 2.

V. DISCUSSION

At first, we find our data approximately $O(4)$ rotational invariant also at $T \neq 0$ as long we consider the confinement phase. The small difference between the corresponding electric and magnetic correlators (both for \mathcal{D}_{\parallel} and \mathcal{D}_{\perp}) probably can be attributed to overlapping fields of (anti)calorons, within a small density expansion. This picture, however, breaks

down in the deconfined phase. In the confinement phase, the correlator $\mathcal{D}_{\parallel}^E$ practically coincides with $\mathcal{D}_{\parallel}^B$ (see Fig. 1 and note there the upward shift by a factor two in the latter). At the transition, the breakdown of $\mathcal{D}_{\parallel}^E$ (in the correlation length) is the most notable result of our analysis.

Comparing the two methods of fitting we find that the condensates estimated from the constrained, purely exponential fits in terms of two structure functions \mathcal{D}^E and \mathcal{D}_1^E tend to be bigger than the condensates from the second fit. This is because the latter better accounts for the real shape of the correlators near zero distance.

The exponential fit also does not properly describe the correlator $\mathcal{D}_{\parallel}^B$ at large distances. This observation holds for all temperatures. Within the deconfined phase, the \mathbf{E} correlators cannot be described at all, by an Ansatz in terms of exponential \mathcal{D}^E and \mathcal{D}_1^E functions. Thus, the rapid change of the exponential correlation lengths (in particular, of the electric correlation length) at the transition merely reflects the difficulty to reach a constrained fit within these assumptions.

The Gauss-exponential fit proves to be much more robust over the whole range of temperatures. Without any further assumptions concerning the shape of $\mathcal{D}^{E,B}$ and $\mathcal{D}_1^{E,B}$, such a fit gives access to these functions which indeed seem to be poorly described by exponentials. We have to describe them by integrated correlation lengths which cannot be directly compared with the exponential correlation lengths of the supposedly exponential fits. In general, the integrated correlation lengths turn out to be bigger than the exponential ones.

In contrast to the exponential correlation lengths of the constrained exponential fits, the integrated correlation lengths associated to the correlation functions $\mathcal{D}^{E,B}$ and $\mathcal{D}_1^{E,B}$, as reconstructed from the second fit, change rather smoothly. As the result of these smooth changes with temperature, the correlation function $\mathcal{D}_{\parallel}^E$ drops (in correlation length) at the deconfinement transition.

The reconstruction of the absolute size of \mathcal{D} and \mathcal{D}_1 structure functions (condensates) from the fits of \mathcal{D}_{\parallel} and \mathcal{D}_{\perp} becomes increasingly difficult at higher and higher temperature. Below the deconfinement temperature and even near to T_{dec} as a characteristic feature of

the data, it is well-recognized, that the \mathcal{D}_1 part of the electric and the magnetic correlator is considerably smaller than the \mathcal{D} part.

The dominance of (anti)selfdual fields, however, associated with this observation is already weaker in our present results, at temperatures below the transition, than it has been found for zero temperature. It is also weaker than what has been found analyzing cooling data for quenched $SU(3)$ near the deconfinement temperature. In Table V this statement can be checked for the so-called non-Abelianicity of the magnetic correlator. It is roughly 80 % at $T = 0.7 T_{\text{dec}}$ and drops to than 70 % at T_{dec} . In the deconfined phase κ^B amounts to approximately 50 %, with an increasing uncertainty.

The positivity of magnetic and electric \mathcal{D}_1 is a clear feature of the data. This applies to the correlators obtained in this work by smoothing as well as to the measurements using the cooling method (for quenched $SU(3)$). Within a caloron analysis (which successfully works only below T_{dec} for the $SU(3)$ cooling data) there is no compelling reason to have $\mathcal{D}_1 < 0$. This is unlike the instanton liquid description for $T = 0$. A caloron analysis of the present data will be given elsewhere [46].

The sum of $\mathcal{D}(0)$ and $\mathcal{D}_1(0)$ is given by the extrapolation to zero distance of both \mathcal{D}_{\parallel} and \mathcal{D}_{\perp} for the electric and magnetic correlators. This quantity is known without big uncertainty and is also presented in Table V in physical units for the six temperatures. The behavior of condensates and correlation lengths is sketched graphically across and beyond the deconfinement transition in Fig. 3. Quantitatively, the correlation lengths are not very different from the results of the cooling method, applied on $SU(3)$ configurations.

The present work dealt with $SU(2)$ pure gauge theory instead of the phenomenologically more interesting case of $SU(3)$. However it has shown an interesting pattern of temperature dependence of the magnetic and electric correlation lengths related to the different structure functions. While the basic structure functions \mathcal{D} and \mathcal{D}_1 change smoothly across the phase transition, the most dramatic effect, the breakdown of $\mathcal{D}_{\parallel}^E$, results from the interplay. A simple picture according to which \mathcal{D}^E would turn to zero in the deconfined phase is not corroborated by our data.

It seems to be worthwhile to investigate the field strength correlators for $SU(2)$ using the cooling method, too, in order to compare it with the smoothing method applied here. It would be even more interesting to implement the RG smoothing method for the gauge group $SU(3)$. This would then allow for a direct comparison with the pioneering results already available thanks to the Pisa group.

TABLES

$w(i, j)$	$j = 1$	$j = 2$	$j = 3$	$j = 4$
$i = 1$ (plaquettes)	1.115504	-0.5424815	0.1845878	-0.01197482
$i = 2$ (6-link loops)	-0.01443798	0.1386238	-0.07551325	0.01579434

TABLE I. Weight coefficients of the simplified fixed-point action for $SU(2)$.

Type	β	T/T_{dec}	A_0/T_{dec}^4	$\Lambda_0 \times T_{\text{dec}}$	A_1/T_{dec}^4	$\Lambda_1 \times T_{\text{dec}}$	$\chi^2/\text{d.o.f.}$
E	1.40	0.71	3.92(2)	0.326(5)	1.59(1)	0.354(1)	15.92
E	1.50	0.90	6.94(5)	0.274(6)	3.09(3)	0.314(1)	10.11
E	1.55	1.02	17.4(8)	0.156(2)	5.016(6)	0.318(1)	10.84
E	1.60	1.15	270(290)	0.055(6)	12.80(4)	0.2520(3)	27.33
B	1.40	0.71	3.50(1)	0.3455(5)	1.45(1)	0.368(1)	7.271
B	1.50	0.90	6.59(3)	0.2920(6)	3.04(3)	0.310(1)	4.526
B	1.55	1.02	7.03(6)	0.2832(7)	4.45(3)	0.290(1)	0.823
B	1.60	1.15	7.41(4)	0.2760(8)	6.51(4)	0.273(1)	0.294
B	1.70	1.47	12.1(1)	0.2386(9)	14.9(1)	0.2272(8)	0.448
B	1.80	1.88	23.2(3)	0.2004(8)	35.2(3)	0.1853(7)	0.660

TABLE II. Condensates and correlation lengths obtained from exponential fits of the form $\mathcal{D}^{E,B}(\mathbf{x}) = A_0 \exp(-|\mathbf{x}|/\Lambda_0)$ and $\mathcal{D}_1^{E,B}(\mathbf{x}) = A_1 \exp(-|\mathbf{x}|/\Lambda_1)$ for various temperatures T . The data was fitted for lattice distances $d > 2a$. Type E refers to \mathcal{D}^E and \mathcal{D}_1^E , type B to \mathcal{D}^B and \mathcal{D}_1^B .

Type	β	A	B	C	$\chi^2/\text{d.o.f.}$
$\mathcal{D}_{\parallel}^E$	1.40	0.039(3)	0.628(2)	0.1372(7)	0.278
\mathcal{D}_{\perp}^E	1.40	0.039(1)	0.6314(7)	0.0503(2)	0.278
$\mathcal{D}_{\parallel}^B$	1.40	0.038(1)	0.5724(6)	0.0599(2)	0.245
\mathcal{D}_{\perp}^B	1.40	0.038(7)	0.570(1)	0.1382(5)	0.245
$\mathcal{D}_{\parallel}^E$	1.50	0.030(3)	0.584(3)	0.137(1)	0.137
\mathcal{D}_{\perp}^E	1.50	0.030(1)	0.5992(9)	0.0444(2)	0.137
$\mathcal{D}_{\parallel}^B$	1.50	0.029(1)	0.5178(7)	0.0584(2)	0.162
\mathcal{D}_{\perp}^B	1.50	0.029(6)	0.525(2)	0.1306(6)	0.162
$\mathcal{D}_{\parallel}^E$	1.55	0.022(8)	0.48(1)	0.255(5)	0.044
\mathcal{D}_{\perp}^E	1.55	0.022(2)	0.623(01)	0.0369(3)	0.044
$\mathcal{D}_{\parallel}^B$	1.55	0.023(1)	0.4972(8)	0.0509(2)	0.070
\mathcal{D}_{\perp}^B	1.55	0.023(3)	0.517(2)	0.1269(7)	0.070
$\mathcal{D}_{\parallel}^E$	1.60	0.015(5)	0.60(1)	0.261(9)	0.083
\mathcal{D}_{\perp}^E	1.60	0.015(2)	0.613(1)	0.0379(3)	0.083
$\mathcal{D}_{\parallel}^B$	1.60	0.019(1)	0.499(7)	0.0406(2)	0.051
\mathcal{D}_{\perp}^B	1.60	0.019(5)	0.616(2)	0.0869(6)	0.051
$\mathcal{D}_{\parallel}^E$	1.70	0.012(3)	0.46(1)	0.411(7)	0.116
\mathcal{D}_{\perp}^E	1.70	0.012(1)	0.634(1)	0.0306(3)	0.116
$\mathcal{D}_{\parallel}^B$	1.70	0.015(1)	0.4902(8)	0.0328(2)	0.042
\mathcal{D}_{\perp}^B	1.70	0.015(1)	0.510(2)	0.1305(9)	0.042
$\mathcal{D}_{\parallel}^E$	1.80	0.095(7)	0.35(1)	0.4867(7)	0.130
\mathcal{D}_{\perp}^E	1.80	0.095(1)	0.6212(9)	0.0291(2)	0.130
$\mathcal{D}_{\parallel}^B$	1.80	0.013(2)	0.5002(7)	0.0258(2)	0.043
\mathcal{D}_{\perp}^B	1.80	0.013(4)	0.539(2)	0.1227(8)	0.043

TABLE III. Parameters from the fit to the raw data of the correlators shown in Fig. 1 in lattice units. The parameters A , B and C correspond to a respective Ansatz for $\mathcal{D}_{\parallel}^{E,B}$ and $\mathcal{D}_{\perp}^{E,B}$, $\mathcal{D}(\mathbf{x}) = A \exp(-B |\mathbf{x}| - C |\mathbf{x}|^2)$.

β	T/T_{dec}	$\mathcal{D}^E(0)/T_{\text{dec}}^4$	$\mathcal{D}^B(0)/T_{\text{dec}}^4$	$\mathcal{D}_1^E(0)/T_{\text{dec}}^4$	$\mathcal{D}_1^B(0)/T_{\text{dec}}^4$	$\xi_{\text{int}}^B \times T_{\text{dec}}$	$\xi_{\text{int}}^E \times T_{\text{dec}}$
1.4	0.71	2.00(5)	2.0(1)	0.54(6)	0.52(3)	0.44(3)	0.42(2)
1.5	0.90	3.9(2)	3.7(3)	1.1(1)	1.2(3)	0.38(1)	0.34(2)
1.55	1.02	4.9(4)	4.4(2)	1.1(6)	2.0(2)	0.35(2)	0.25(3)
1.6	1.15	3.6(4)	4.4(6)	3.1(4)	4.2(7)	0.27(4)	0.24(4)
1.7	1.47	8.4(7)	8.1(16)	5.2(8)	5.5(23)	0.25(3)	0.15(3)
1.8	1.88	20.1(57)	22.0(20)	9.9(59)	19.0(24)	0.20(2)	0.10(3)

TABLE IV. Condensates and integrated correlation lengths of $\mathcal{D}^{E,B}$ for the fit presented in Table III for various temperatures T . All quantities are expressed in comparison to T_{dec} .

β	$\mathcal{D}^E(0) + \mathcal{D}_1^E(0)$ [GeV ⁴]	$\mathcal{D}^B(0) + \mathcal{D}_1^B(0)$ [GeV ⁴]	κ^B	σ^B [GeV ²]
1.4	0.020(1)	0.020(1)	0.79(3)	0.10(1)
1.5	0.039(2)	0.039(4)	0.75(5)	0.14(3)
1.55	0.047(8)	0.051(3)	0.69(15)	0.14(3)
1.6	0.053(7)	0.068(10)	0.51(41)	0.15(5)
1.7	0.107(12)	0.107(30)	0.60(23)	0.15(10)
1.8	0.237(92)	0.323(34)	0.54(64)	0.27(19)

TABLE V. Some physically interesting quantities (for $SU(2)$) in physical units. The magnetic string tension σ^B is given by (10) in terms of \mathcal{D}^B . For definiteness, we took $T_{\text{dec}} = 0.298$ GeV for pure $SU(2)$ gauge theory.

FIGURES

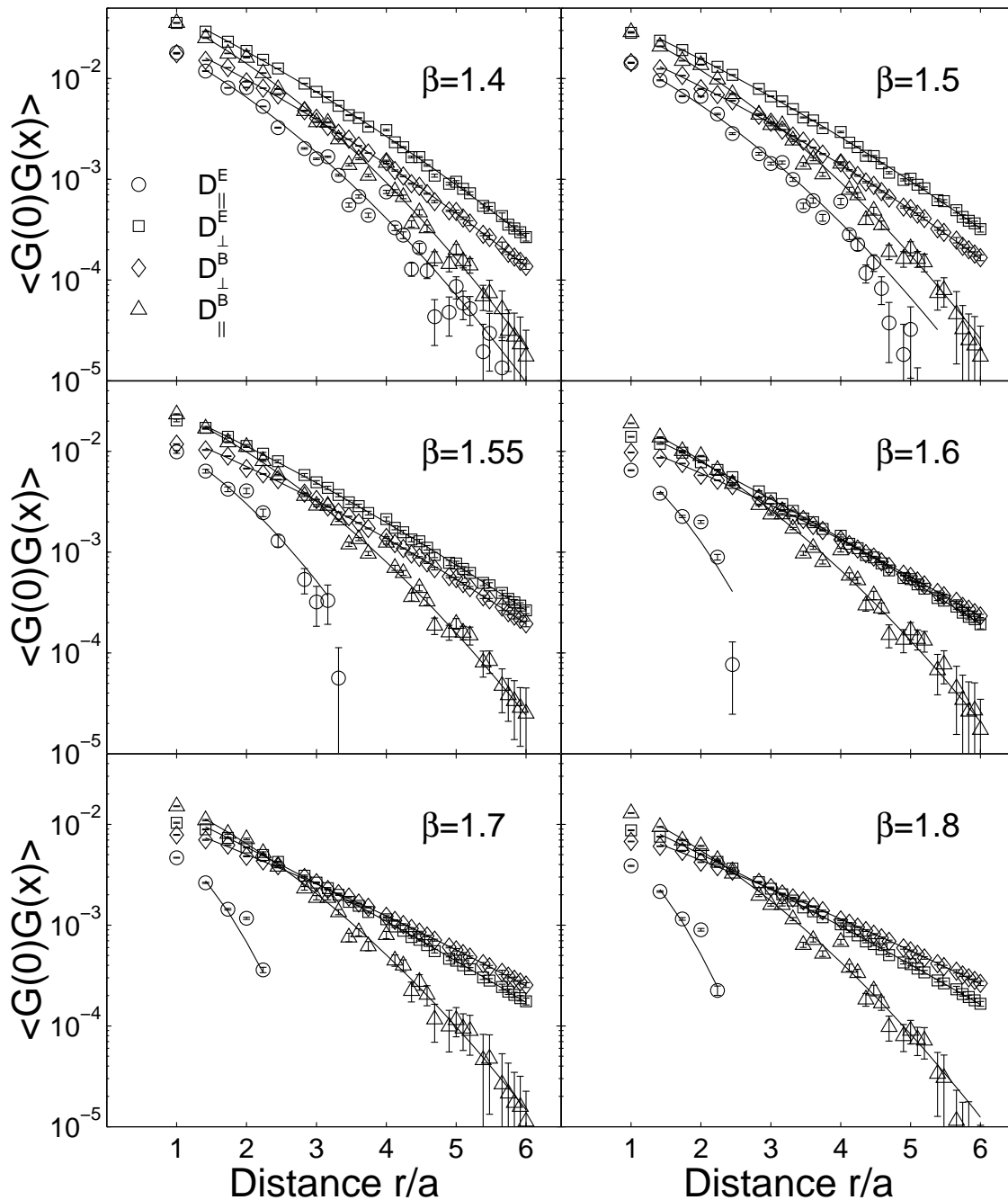


FIG. 1. Raw correlator data fitted according to a generic form $A \exp(-B|x| - C|x|^2)$. The corresponding fit parameters are reported in Table III. Errors are determined by the jackknife method for a block size of 100. The dependence on the block size was found to be marginal. For the clarity of the plot the data and curves shown for D_{\perp}^E and D_{\parallel}^B include a factor two shift upward.

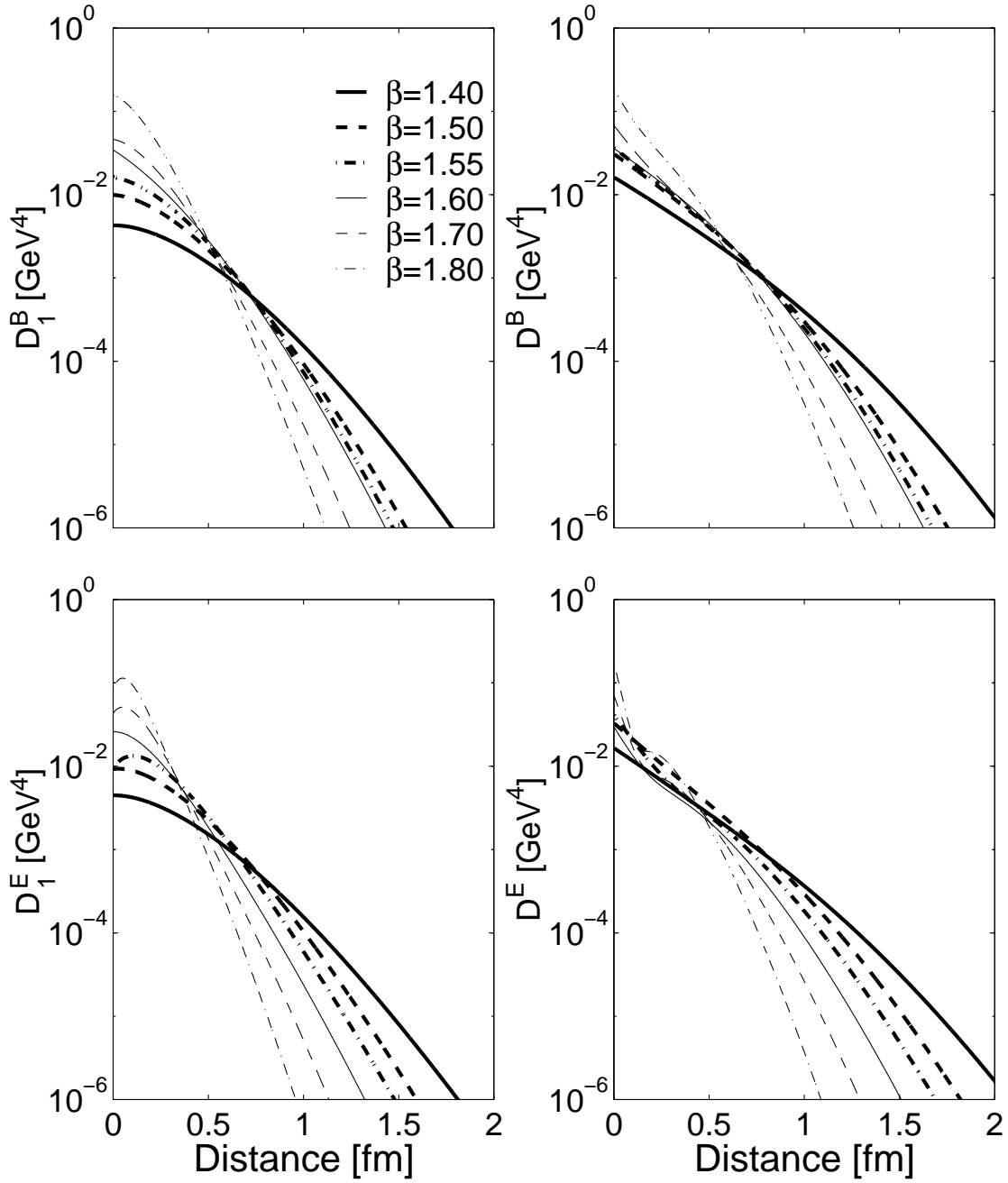


FIG. 2. $\mathcal{D}^{E,B}$ and $\mathcal{D}_1^{E,B}$ reconstructed from the Gauss-exponential fit of Fig. 1 and Table III, here presented in physical units.

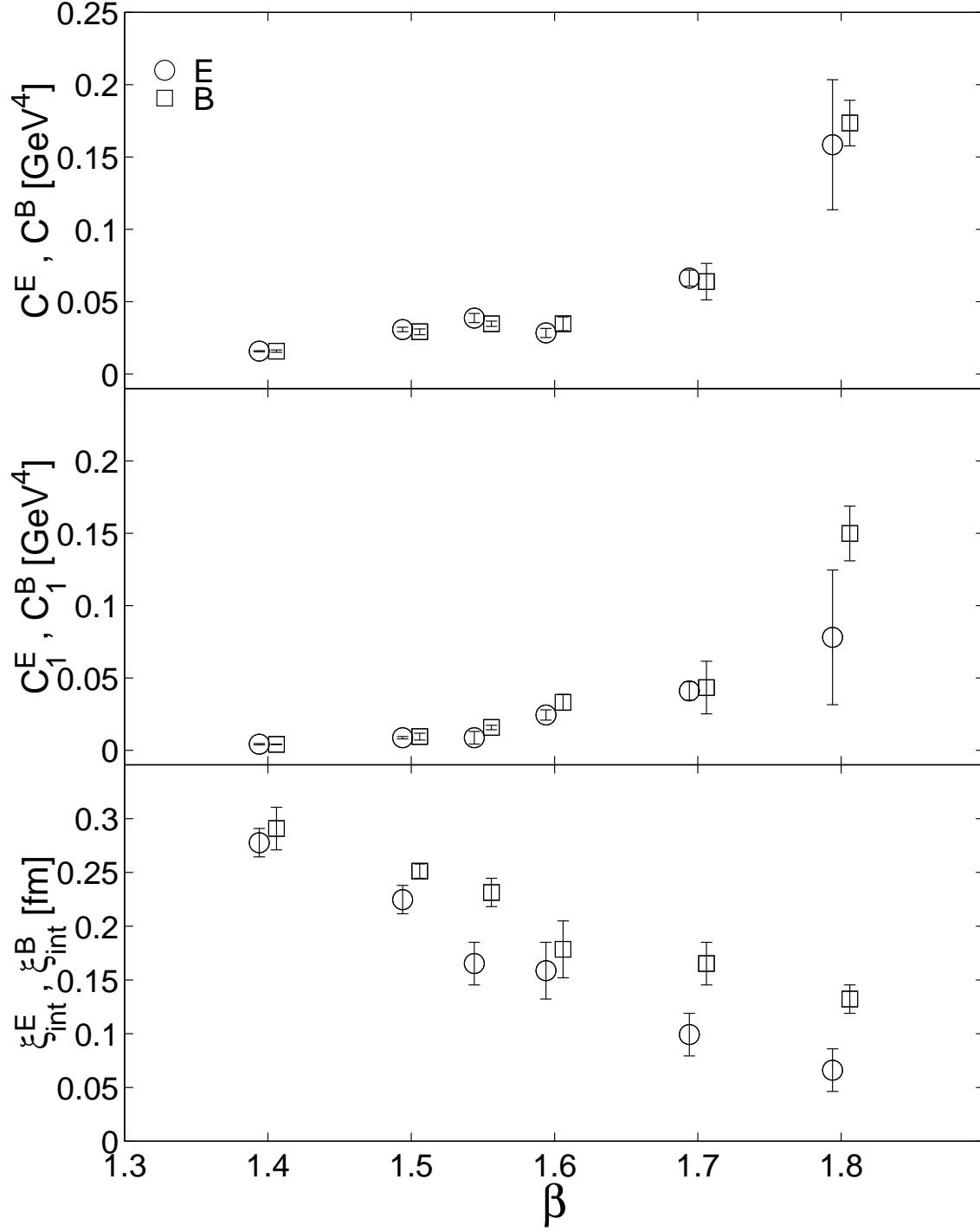


FIG. 3. Condensates and correlation lengths as listed in Table IV, here expressed in physical units and shown *vs.* β .

REFERENCES

- [1] Confinement and topology session in *Lattice '98*, to appear in Nucl. Phys. (Proc. Suppl.) (1999).
- [2] H. G. Dosch, Phys. Lett. **B190**, 177 (1987); H. G. Dosch and Yu. A. Simonov, Phys. Lett. **B205**, 339 (1988); Yu. A. Simonov, Nucl. Phys. **B324**, 67 (1989).
- [3] Yu. A. Simonov, Usp. Fiz. Nauk **166**, 337 (1996); Phys. Usp. **39**, 313 (1996).
- [4] D. Gromes, Phys. Lett. **B115**, 482 (1982); M. Campostrini, A. Di Giacomo, Š. Olejnik, Z. Phys. C **31**, 577 (1986); Yu. A. Simonov, S. Titard, and F. J. Yndurain, Phys. Lett. **B354**, 435 (1995).
- [5] P. V. Landshoff and O. Nachtmann, Z. Phys. C **35**, 405 (1987); O. Nachtmann, Ann. Phys. (NY) **209**, 436 (1991); A. Krämer and H. G. Dosch, Phys. Lett. **B252**, 669 (1990); H. G. Dosch, E. Ferreira, and A. Krämer, Phys. Rev. D **50**, 1992 (1994); A. F. Martini, M. J. Menon, and D. S. Thober, Phys. Rev. D **57**, 3026 (1998).
- [6] M. Campostrini, A. Di Giacomo, and G. Mussardo, Z.Phys. C **25**, 173 (1984).
- [7] A. Di Giacomo and H. Panagopoulos, Phys. Lett. **B285**, 133 (1992).
- [8] A. Di Giacomo, E. Meggiolaro, and H. Panagopoulos, Nucl. Phys. **B** (Proc. Suppl.) **54 A**, 343 (1997).
- [9] A. Di Giacomo, E. Meggiolaro, and H. Panagopoulos, Nucl. Phys. **B483**, 371 (1997).
- [10] M. D'Elia, A. Di Giacomo, and E. Meggiolaro, Phys. Lett. **B408**, 315 (1997); e-print Archive: hep-lat/9809055.
- [11] E.-M. Ilgenfritz, B. V. Martemyanov, S. V. Molodtsov, M. Muller-Preussker, and Yu. A. Simonov, Phys. Rev. D **58**, 114508 (1998).
- [12] E. V. Shuryak and J. J. M. Verbaarschot, Nucl. Phys. **B410**, 37, 55 (1993); T. Schäfer, E. V. Shuryak, and J. J. M. Verbaarschot, Nucl. Phys. **B412**, 143 (1994).

- [13] T. Schäfer and E. V. Shuryak, *Rev. Mod. Phys.* **70**, 323 (1998).
- [14] D. Chen, R. C. Brower, J. W. Negele, and E. Shuryak, e-Print Archive: hep-lat/9809091.
- [15] E.-M. Ilgenfritz and S. Thurner, e-Print Archive: hep-lat/9810010.
- [16] D. Diakonov and V. Petrov, e-Print Archive: hep-lat/9810037.
- [17] T. DeGrand, A. Hasenfratz, and T. Kovacs, *Nucl. Phys.* **B505**, 417 (1997).
- [18] M. Fukushima, H. Suganuma, and H. Toki, e-Print Archive: hep-lat/9902005.
- [19] T. Suzuki, *Prog. Theor. Phys.* **80**, 929 (1988); S. Maedan and T. Suzuki, *Prog. Theor. Phys.* **81**, 229 (1989).
- [20] M. Baker, N. Brambilla, H. G. Dosch, and A. Vairo, *Phys. Rev. D* **58**, 034010 (1998).
- [21] U. Ellwanger, *Eur. Phys. J.* **C7**, 673 (1999).
- [22] E.-M. Ilgenfritz, B. V. Martemyanov, M. Müller-Preussker, in preparation.
- [23] M. Feurstein, E.-M. Ilgenfritz, M. Müller-Preussker, and S. Thurner, *Nucl. Phys.* **B511**, 421 (1998).
- [24] E.-M. Ilgenfritz, H. Markum, M. Müller-Preussker, and S. Thurner, *Phys. Rev. D* **58**, 094502 (1998).
- [25] E. Meggiolaro, e-Print Archive: hep-ph/9807567.
- [26] V. I. Shevchenko and Yu. A. Simonov, *Yad. Fiz.* **60**, 1329 (1997); *transl. Phys. Atom. Nucl.* **60**, 1201 (1997).
- [27] V. I. Shevchenko and Yu. A. Simonov, *Phys. Lett.* **B437**, 131 (1998).
- [28] A. E. Dorokhov, S. V. Esaibegyan, and S. V. Mikhailov, *Phys. Rev D* **56**, 4062 (1997).
- [29] D. I. Diakonov and V. Yu. Petrov, *Nucl. Phys.* **B245**, 259 (1984).
- [30] A. E. Dorokhov, S. V. Esaibegyan, A. E. Maximov, and S. V. Mikhailov, e-Print Archive:

hep-ph/9903450

- [31] Yu. A. Simonov, JETP Lett. **54**, 249 (1991); JETP Lett. **55**, 627 (1992).
- [32] B. J. Harrington, and H. K. Shepard, Phys. Rev. D **17**, 2122 (1978).
- [33] D. J. Gross, R. D. Pisarski, L. G. Yaffe, Rev. Mod. Phys. **53**, 43 (1981).
- [34] L. Del Debbio, A. Di Giacomo, and Yu. A. Simonov, Phys. Lett. **B332**, 111 (1994).
- [35] G. Bali, N. Brambilla, and A. Vairo, Phys. Lett. **B421**, 265 (1998).
- [36] T. DeGrand, A. Hasenfratz, and T. G. Kovacs, Nucl. Phys. **B520**, 301 (1998).
- [37] D. A. Smith and M. J. Teper, Phys. Rev. D **58**, 014505 (1998).
- [38] P. de Forcrand, M. Garcia Perez, and I. O. Stamatescu, Nucl. Phys. **B47** (Proc. Suppl.) **47**, 777 (1996); Nucl. Phys. **B53** (Proc. Suppl.) **53**, 557 (1997); Nucl. Phys. **B499**, 409 (1997).
- [39] J. W. Negele, in *Lattice '98*, e-Print Archive: hep-lat/9810053.
- [40] M. Garcia Perez, O. Philipsen, and I.-O. Stamatescu, e-Print Archive: hep-lat/9812006.
- [41] E.-M. Ilgenfritz, H. Markum, M. Müller-Preussker, and S. Thurner, e-Print Archive: hep-lat/9904010.
- [42] T. Suzuki, Prog. Theor. Phys. Suppl. **131**, 633 (1998).
- [43] T. A. DeGrand, A. Hasenfratz, and De-cai Zhu, Nucl. Phys. **B475**, 321 (1996); Nucl. Phys. **B478**, 349 (1996).
- [44] T. G. Kovacs, private communication.
- [45] T. DeGrand, A. Hasenfratz, P. Hasenfratz, and F. Niedermayer, Nucl. Phys. **B454**, 587 (1995); Nucl. Phys. **B454**, 615 (1995).
- [46] E.-M. Ilgenfritz, B. V. Martemyanov, M. Müller-Preussker, and S. Thurner, in prepa-

ration.